Opened-Ring Electrode Array for Enhanced Non-invasive Monitoring of Bioelectrical Signals: Application to Surface EEnG Recording

J. Garcia-Casado[1(✉)], V. Zena[1], J.J. Perez[1], G. Prats-Boluda[1], Y. Ye-Lin[1], and E. Garcia-Breijo[2]

[1] Grupo de Bioelectrónica, CI2B-UPV, Camino de Vera SN, 46022 Valencia, Spain
{jgarciac, vfzena, jjperez, gprats, yiye}@gbio.i3bh.es
[2] Centro de Reconocimiento Molecular y Desarrollo Tecnológico, Ud. Mixta UPV-UV, Camino de Vera SN, 46022 Valencia, Spain
egarciab@eln.upv.es

Abstract. The estimation of Laplacian potential on the body surface obtained by means of concentric ring electrodes can provide bioelectrical signals with better spatial resolution and less affected by bioelectrical interferences than monopolar and bipolar recordings with conventional disc electrodes. In this paper an array of flexible concentric opened-ring electrodes for non-invasive bioelectrical activity recordings is presented. A preconditioning circuit module is directly connected to the electrode array to perform a first stage of filtering and amplification. A computer model reveals differences minor than 1 % between the sensitivity of the proposed opened-ring electrode vs a closed-ring electrode. Simultaneous recordings of intestinal myoelectrical activity proved that signals from the developed array of electrodes presented lower electrocardiographic and respiratory interference than conventional bipolar recordings with disc electrodes. The small bowel's slow wave myoelectrical activity can be identified more easily in the recordings with the presented ringed-electrodes.

Keywords: Ring electrode · Laplacian recording · Non-invasive myoelecrical recording · Electroenterogram

1 Introduction

1.1 Bioelectrical Laplacian Recordings

Surface recordings of bioelectrical signals are usually recorded by means of disc electrodes in bipolar or unipolar configuration. In the first method the potential difference between a pair of electrodes is measured. In the latter method the potential of each electrode is compared either to a neutral electrode or to the average of several electrodes. One drawback of using conventional disc electrodes in bioelectrical surface recordings is their poor spatial resolution which is mainly caused by the blurring effect of the different conductivities of the volume conductor [1]. In this respect, Laplacian has been

M. Fernández-Chimeno et al. (Eds.): BIOSTEC 2013, CCIS 452, pp. 26–40, 2014.
DOI: 10.1007/978-3-662-44485-6_3

shown to reduce the smoothing effects caused by the volume conductor and to increase the spatial resolution in localizing and differentiating multiple dipole sources [2, 3].

There are different approaches to estimate the Laplacian potential on the body surface. The first ones to be used were discretization techniques like the one introduced by Hjorth as early as in 1975 [4]. In that study, the Laplacian of the EEG signal was estimated as the difference between the average potential of four disc electrodes in the form of a cross and the potential of a fifth disc electrode placed in the center of the cross. In the late 80 s, analytic solutions to estimate the Laplacian of the surface potential were proposed in order to reduce discretization errors [5]. These are complex discrete computational techniques, generally not suitable for real-time applications. Nevertheless, Laplacian potential can also be directly estimated by means of concentric ring electrodes in tripolar, bipolar or tripolar in bipolar configuration (TCB, where the outer ring and the center disc were electrically shorted) [3, 6, 7].

Ring electrodes have already been used to estimate the Laplacian potential of bioelectrical signals such as the electrocardiogram (ECG), electroencephalogram (EEG), electroenterogram (EEnG) and the electrohysterogram (EHG), so as to increase the spatial resolution of and the signal quality of conventional surface potential recordings [6–9]. These electrodes are usually active since the signals sensed by concentric ring electrodes in Laplacian configuration are weaker than the ones obtained by conventional monopolar or bipolar recordings, and the output impedance is bigger. Nevertheless, the ringed-electrodes used in these studies were developed on rigid substrates like printed-circuit boards, what can provoke a poor skin-to-electrode contact and discomfort to the patient.

Therefore, the aim of this study is to develop concentric ring electrodes on a flexible substrate to join the advantages of Laplacian recordings with the comfort and better adaptation to the body surface curvature of conventional disposable disc electrodes.

1.2 Intestinal Myoelectrical Activity

The study of intestinal motility is an outstanding field in gastroenterology due to the fact that abnormal motility patterns are related with several intestinal pathologies [10]. This is the case in irritable bowel syndrome, intestinal obstruction, paralytic ileus, and bowel ischemia. The main problem in monitoring intestinal activity is the difficult anatomic access, hence most methods of studying this activity are considered to be invasive. One possible solution would be the recording of intestinal myoelectrical activity on abdominal surface. This signal is named Electroenterogram (EEnG) and it is composed of two waves: slow waves (SW) and spike burst (SB). The former are periodical, omnipresent electrical potentials that regulate the maximum rate of intestinal muscle contractions. The latter are fast action potentials which are located in the plateau of the SW. They are only present when contractions appear. Whereas SW are related to the frequency and propagation velocity of the contractions [11], SB determine the presence and the intensity of the contractions. The frequency of the SW changes along the small intestine with a stepwise gradient from about 12 cpm at duodenum to 8 cpm at ileum [12].

There are few studies about abdominal surface recordings to identify the EEnG in humans [9, 13–15]. The main reason is that human EEnG is a very weak signal, which is severely attenuated especially in the SB frequency range, because of the insulation effects of the abdominal layers and spatial filtering [1, 16]. Surface EEnG is also very sensitive to physiological interferences such as ECG and respiration, being difficult to identify the SW component of the EEnG by visual inspection of abdominal surface recordings. The ECG spectral frequency range overlaps the SB frequency range, therefore it is necessary to eliminate it from abdominal recordings to identify the SB component of the EEnG [17]. As regards to respiration interference, the typical breathing frequency range (12 cpm to 24 cpm) is very close to the frequency of the SW (8 cpm to 12 cpm), so it is not possible to use conventional filters to remove this interference.

Laplacian recordings of the EEnG by means of active concentric ring electrodes on rigid substrates have proven to enhance signal quality in comparison to conventional monopolar and bipolar recordings with disc electrodes [9]. Therefore, a second objective of this work is to test and study the possible benefits of the flexible concentric ring electrodes to be developed in this study, on the surface recordings of the EEnG.

2 Materials and Methods

2.1 Active Electrode Array Design and Implementation

Sensing Part. In this work it has been decided to design an array of electrodes rather than an individual electrode for surface bioelectrical recordings, since this kind of recordings are usually multichannel and moreover Laplacian recordings are often used for body surface mappings. Specifically an array of three concentric ring TCB active electrodes was developed. The sensor is made out of two parts: a disposable sensing part with three TCB electrodes and a reusable battery-powered signal conditioning circuit. Each of the three sensing electrodes consists of an inner disc and two concentric rings in bipolar configuration i.e. the disc and the outer ring are shorted together.

The outer diameter of the external ring was set to 24 mm which is a compromise between bigger electrodes that would yield signals of higher amplitude and smaller electrodes that would provide better spatial resolution. The rest of dimensions of the electrode are designed considering the following criteria:

- The sum of the areas of the outer ring and the inner disc should be equal to the area of the middle ring so as to provide similar input impedances, improving the common mode rejection ratio.
- The distance between the inner disc and the middle ring should be the same as the distance between the middle and outer rings to reduce common mode interferences.

The dimensions of each ringed-electrode of the array are shown in Fig. 1. As it can also be appreciated in this figure, an opened-ring version has been designed in order to avoid shorts in the single layer layout of the tracks from the electrodes to the connectors. The flexible electrode array was implemented by screen-printing technology on polymer substrates. Specifically, a biocompatible silver paste was printed (Dupont

5064 Silver conductor, thickness 17 μm) on Polyester Melinex ST506 substrate (thickness 175 μm). The serigraphy was made by using an AUREL 900 High precision screen stencil printer. Cured period of inks was 130 °C for 10 min.

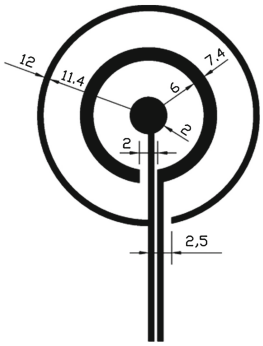

Fig. 1. Dimensions (mm) of the concentric ring electrode to be implemented in the array.

Signal Conditioning Part. As stated before, signals from concentric ring electrodes are of very low amplitude, especially in the cases that the bioelectrical signal to be recorded on the body surface is weak. Therefore it is highly recommended to include an amplification stage as close as possible to the sensing electrode.

In this work a battery-powered conditioning circuit was developed and directly connected to the electrode array. Precisely, a 12 bias (only six are used) flexible-flat-cable-to-flexible-printed-circuit connector (TE Connectivity/AMP-1-84953-2 FFC/FPC) was used for the connection. The circuit is composed of a preamplifier (gain 31.9), followed by a coupling circuit (high pass cut off frequency 0.05 Hz) and an additional differential amplification stage (gain 106.1) for each of the three TCB electrodes of the array. Specifically, the integrated circuits used were 3 OP747 for the operational amplifiers and 3 AD620 for the instrumentation amplifiers. The signal conditioning circuit weights less than 15 g. Its main electrical characteristics were experimentally checked and are shown in the next section.

2.2 Model of the Electrode and Abdomen

In order to compare the sensitivity map of the proposed opened-ring version of the TCB electrode with that of the conventional closed-ring electrode for abdominal recordings, both electrodes and the underlying tissue were modeled and solved by numeric methods.

Similar to the work of Bradshaw et al. [1], the abdomen was modeled as a semi-infinite electric conductor domain composed by five homogeneous and isotropic layers of tissues with its own electrical conductivity (σ) and thickness (th), which represent: skin (th_1 = 5 mm, σ_1 = 0.45 S/m), fat (th_2 = 12 mm, σ_2 = 0.02 S/m), muscle (th_3 = 5 mm, σ_3 = 0.45 S/m), omentum (th_4 = 5 mm, σ_4 = 0.02 S/m) and abdominal cavity (th_5 = 200 mm, σ_5 = 0.45 S/m). Model width and depth were chosen large

enough to ensure a negligible influence of the model's lateral limits on the results. The model of the abdomen can be seen on the bottom of Fig. 2.

So as to accurately compare the results obtained from the geometrical model of the abdomen solved by finite element methods when testing the different types of ring electrodes, it is recommendable that the mesh of the model stays the same. This would permit to get the solutions at fixed spatial coordinates inside the model. However, the mesh and node coordinates are consequence of the geometric characteristic of the model. Therefore, since the geometry of the electrodes to study is different, the mesh will be. To overcome this problem, a unique geometrical model composed by four sets of pieces was used to represent all the electrodes under study in such a way that the electrical conductivity of each one of these pieces was changed between 'High' (conductor, σ_c = 1e5 S/m) and 'Low' (insulator, σ_i = 1e−5 S/m), depending on the geometry of the electrode to be analyzed. The geometrical model of the electrodes with the four sets of pieces is shown on the top of Fig. 2.

Three different types of concentric ring electrodes were studied; and the 'Low' or 'High' conductivity of each of their four sets of pieces is shown in Table 1. The combination of the first row (CRE) yields a closed-ring TCB electrode that could be considered our reference and gold standard. The combination of the second row (ORE_A) and the third row (ORE_B) yield opened-ring TCB electrodes similar to that shown in Fig. 1. In the case of ORE_A the conductive track that shortcuts the inner disc and the outer ring is in contact with the skin, whereas in the case of ORE_B it is not. It can also be deduced that ORE_B is identical to CRE but with opened rings.

Since results obtained from these electrodes are expected to be very similar, once the geometry and material properties of the model were defined, it was meshed with a very high density of elements (>3 million) to minimize errors in the comparison.

The objective was to compare the sensitivity of each electrode to measure the activity of an electrical dipole located inside the abdominal cavity. For this purpose, it has been shown [18] that the voltage between a pair of electrodes A and B caused by an electrical dipole placed at C, is the scalar product of the electric field on C caused by the injection of a unit current between electrodes A and B, and the dipole vector. From this point of view, the sensitivity of the ring electrodes to measure the electrical activity of a dipole inside the abdominal cavity can be approached to the module of the electric field caused by the injection of a unit current between the ring electrodes.

Electrodes and abdomen were modeled and solved by ANSYS (R).

2.3 Signal Recordings

The study was approved by Committee of Ethics of Universidad Politécnica de Valencia. Five recording sessions, of about three hours, were carried out in healthy human volunteers in fast state (>8 h). Subjects were in a supine position inside a Faraday cage. Firstly the abdominal body surface was exfoliated to remove dead skin cells to reduce contact impedance. The abdominal surface was also shaved in male subjects. Figure 3, shows the location of electrodes for the EEnG recordings. The developed flexible electrode array was placed horizontally 2.5 cm below the umbilicus, providing three Laplacian signals. Three monopolar Ag-AgCl floating gel electrodes of

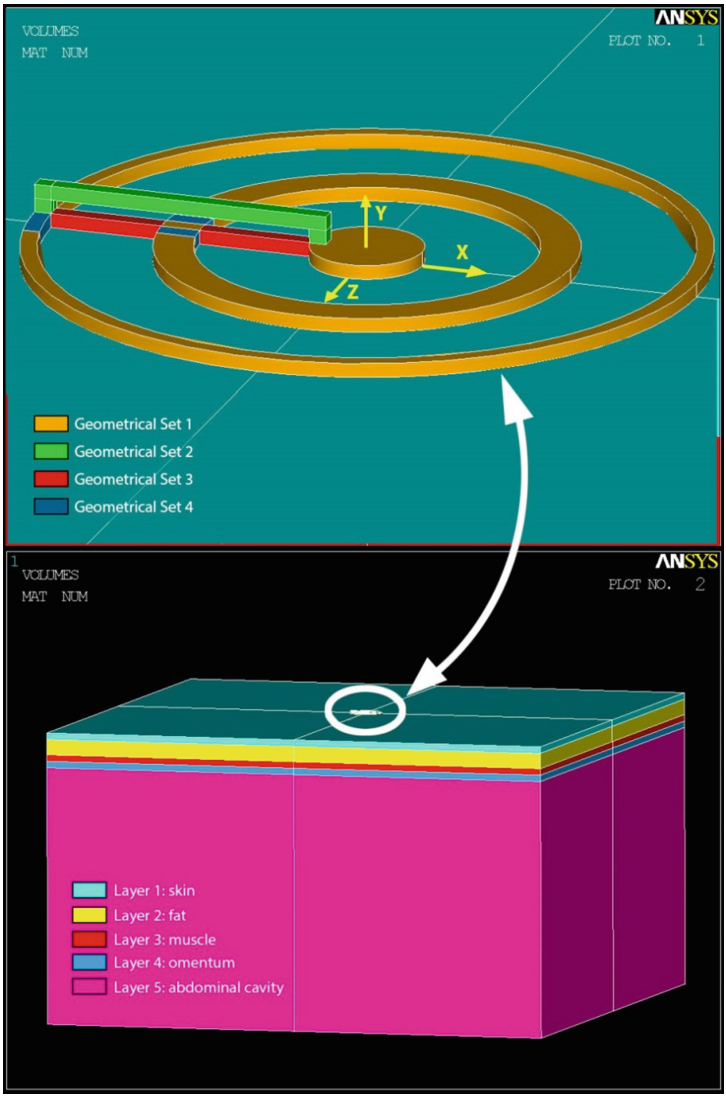

Fig. 2. Model of the electrode (top) and of the abdomen (bottom).

Table 1. Conductivities of the geometrical sets of pieces that conform the electrodes to be tested by the finite elements model. (CRE: closed-ring electrode, ORE: open ring electrode).

Electrode	Geometrical set			
	1	2	3	4
CRE	High	High	Low	High
ORE_A	High	Low	High	Low
ORE_B	High	High	Low	Low

8 mm of sensing diameter (EL258S, Biopac Systems Inc, Santa Barbara, CA, USA) were placed 2.5 cm above the umbilicus. Interelectrode distance was also 2.5 cm. Two bipolar recordings of EEnG were obtained from adjacent monopolar electrodes.

The main sources of physiological interferences usually present on surface EEnG were simultaneously recorded. Specifically, ECG was monitored by Lead 1 using disposable electrodes (EL501, Biopac Systems Inc, Santa Barbara, CA, USA), respiration was recorded by an airflow transducer (1401G, Grass Technologies, Warwick, USA) and body movements were measured by a 3-axis accelerometer (ADXL 335, Analog Devices, LM, Ireland).

All signals, except from acceleration signals, were amplified and band-pass filtered (0.1–100 Hz) by means of commercial bioamplifiers (P511, Grass Technologies, Warwick, USA). A disposable electrode placed on the left ankle of the subject was used as reference for the bioelectrical recordings. Signals were simultaneously recorded at a sampling rate of 1 kHz.

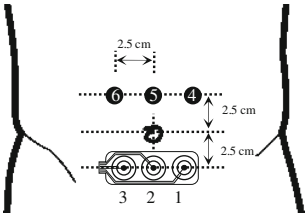

Fig. 3. Location of electrodes for EEnG recordings.

2.4 Signal Analysis

In order to study the activity of the low-frequency component of the EEnG i.e. the slow wave, EEnG and respiratory signals were low-pass filtered (fc = 0.5 Hz) and resampled at 4 Hz.

The power spectral density (PSD) of signals was estimated by means of autoregressive parametrical techniques (AR, order 120). PSD was estimated for moving windows of 120 s every 15 s of the recorded signals. The dominant frequency (DF) over 8 cpm of the PSD of every window was determined. The parameter %Resp was defined as the ratio between the number of windows in which the DF of the surface signal (bipolar or Laplacian) is within the DF of respiration ±0.5 cpm and the total number of windows. Similarly, %TFSW is defined as the ratio of analysed windows whose DF is inside the typical frequency range of intestinal slow wave (8-12 cpm). The rest of cases are included in the parameter %Other.

3 Results

3.1 Sensitivity Map of Opened-Ring Vs Closed-Ring TCB Electrode

Figure 4 displays the normalized spatial distribution on the abdominal cavity of the modulus of the electric field in a radial plane of the CRE. As it could be expected, the

sensitivity is maxima at the point closest to the electrode, and presents a decreasing gradient as we move away from the electrode. For this specific electrode, the effect of the connecting track is negligible and the same sensitivity map is obtained for any other radial plane. Analogous sensitivity maps were obtained for ORE_A and ORE_B electrodes which are not shown since no great differences can be found by visual inspection and to reasons of space.

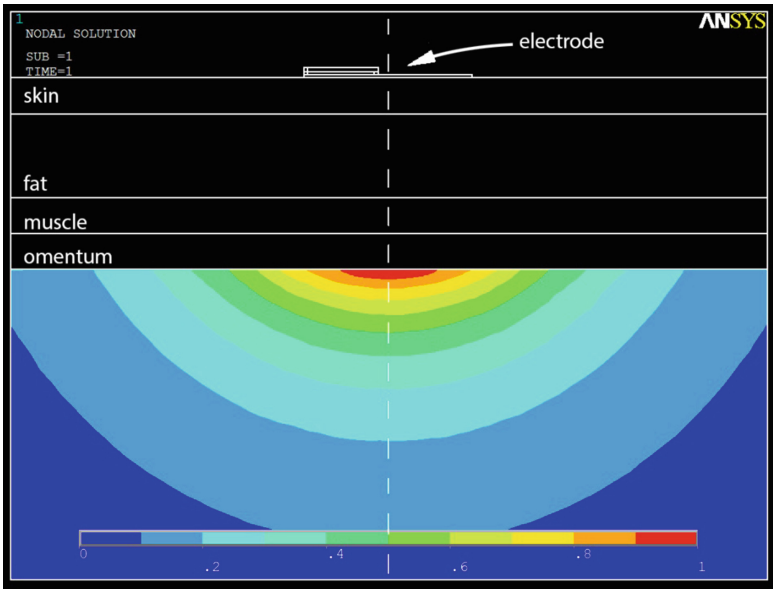

Fig. 4. Normalized spatial distribution of the modulus of the electric field in a radial plane of the closed-ring electrode (CRE).

Table 2 shows the results of the parameters used to describe and compare the sensitivity maps of the three modeled ring electrodes. The results from the model yield that the maximum magnitude of the induced electric field in the abdominal cavity (E_{max}) is almost equal for CRE and ORE_B, but is smaller for ORE_A. This reveals a non-negligible difference in the amplitude of the signals that this kind of electrode would pick-up. Nevertheless, the most important aspect of coaxial ring electrodes is the spatial distribution of its sensitivity which makes them suitable to estimate the Laplacian potencial. Thus, the maximum differences between the normalized spatial distributions of the sensitivity (modulus of the electric field) were obtained and are shown in Table 2. Again, ORE_B presents the most similar spatial distribution of the normalized sensitivity to CRE, providing an error minor than 0.5 %. In the case of ORE_A, in which the connecting track was in contact with the skin, this error is still low but almost reaches a value of 3.8 %.

Table 2. Parameters derived from the sensitivity maps of the modeled electrodes: E_{max} maximum value of the electric field in the abdominal cavity, Δ_{NSD} difference between normalized spatial distribution of the electric field of CRE and ORE.

Electrode	E_{max}(V/m)	Δ_{NSD} (%)	
		Min.	Max.
CRE	4.434	–	–
ORE_A	3.809	−0.46	0.44
ORE_B	4.406	−3.78	3.65

3.2 Active Electrode Array

Figure 5 shows the sensing part of the array of active concentric ring TCB electrodes. It can be appreciated that the substrate is flexible enough to fit the body surface curvature. Moreover the adhesion of the conductor paste to the substrate was checked by means of a sticky tape (8915 Filament APT, 3 M). The paste took off after more than 30 cycles proving the good adherence.

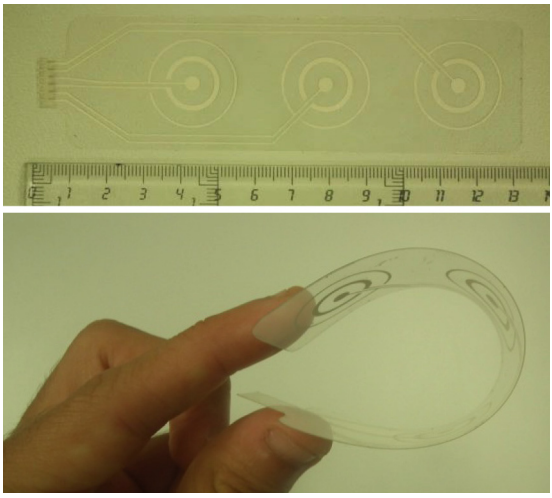

Fig. 5. Implemented flexible array of three TCB concentric ring electrodes.

Both sides of the signal preconditioning circuit of the active electrode array can be seen in Fig. 6. The small size and weight of the circuit and the flexible nature of the array makes it possible to place this part above the electrodes. With the proper fixing strategy, the active electrode array could be used for ambulatory monitoring. Table 3 summarizes the main electrical characteristics of the developed signal conditioning circuit. It can be observed that the battery life is adequate for the recording sessions, and the CMRR and output noise are also appropriate for bioelectrical applications.

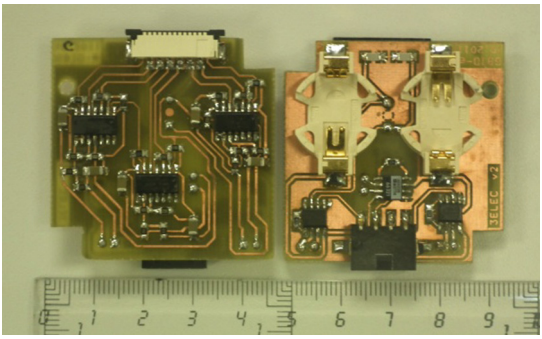

Fig. 6. Signal preconditioning circuit: bottom side (left) and top side (right).

Table 3. Main electrical parameters of the signal-preconditioning circuit.

1	0.049 Hz
Differential gain at medium frequency	3386 V/V
CMRR at medium frequencies	116 dB
CMRR at 50 Hz	103 dB
Output noise	0.195 mVrms
Battery life	280 min

3.3 EEnG Monitoring

Figure 7 shows an example of the biosignals simultaneously recorded. It can be appreciated that, as expected, the amplitude of the signals picked up by the ringed-electrodes of the array is smaller than that of the bipolar recordings with disc electrodes. Nevertheless, the conventional bipolar recordings present stronger ECG interference as it can be easily observed in this figure. In the signals from concentric ring electrodes the electrocardiographic interference is almost null. It can only be hardly appreciated in the signal corresponding to electrode 1 (Lp1) which is placed on the left side of the subject. Regarding the intestinal SW activity, approximately five waves can be identified on the Laplacian recordings. In bipolar recordings this is difficult to identify by visual inspection since it seems they are strongly corrupted by the respiration. This can also be observed in the example of PSD of signals shown in Fig. 8. In bipolar recordings the dominant frequency (DF) corresponds to the respiratory frequency; whereas the DF of Laplacian recordings is around 10.5 cpm which fits the normal SW frequency in human jejunum.

The results of the %TFSW, %Resp and %Other parameters, which are presented in Table 4, confirm this behavior. It is shown that in around 25 % of the signal windows studied, the respiratory interference masks the intestinal SW activity. In contrast, this ratio is only around 10 % for the Laplacian recordings. Furthermore, around 75 % of the cases the DF of Laplacians recordings the DFs are in the frequency range associated to the intestinal SW, whereas it is about 65 % for the conventional bipolar recordings.

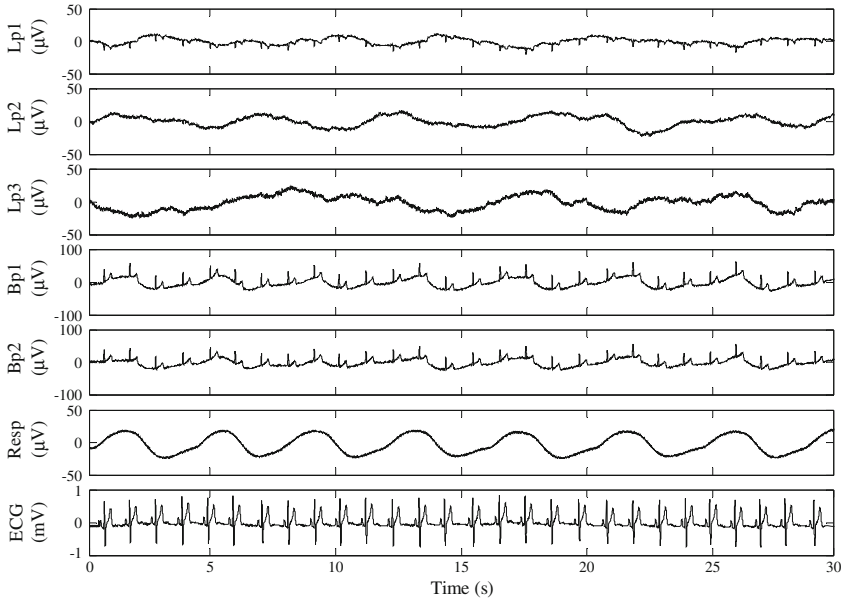

Fig. 7. Simultaneous recording of biosignals: Lp1–3: Laplacian signals from the electrode array; Bp1–2: bipolar signals from disc electrodes; Resp: respiration; ECG: electrocardiogram.

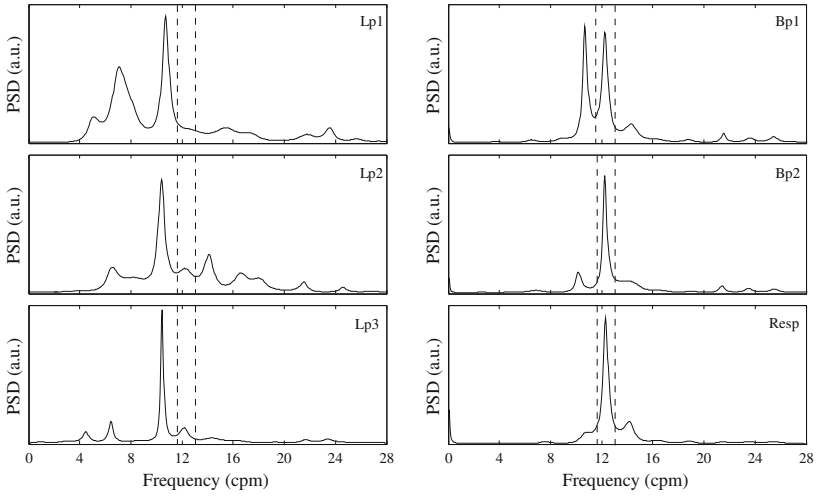

Fig. 8. Example of power spectrum density (AR120) of a 120 s window of recorded biosignals. The bandwidth associated to respiratory components is represented in dashed lines.

Finally to say that the number of cases whose DF is associated to SW harmonics or other components is slightly higher in Laplacian recordings than in conventional bipolar recordings.

Table 4. Percentage of dominant frequency in the bandwidths of the different components (mean ± standard deviation); N = 3385, Lp1–3: Laplacian signals from the electrode array, Bp1–2: bipolar signals from disc electrodes.

Channel	%TFSW	%Resp	%Other
Lp1	76,6 ± 8,6	11,3 ± 5,6	12,0 ± 5,8
Lp2	72,8 ± 8,2	9,5 ± 7,0	17,7 ± 6,2
Lp3	71,2 ± 6,9	11,6 ± 8,0	17,2 ± 3,8
Bp1	63,0 ± 12,1	27,3 ± 12,0	9,7 ± 4,8
Bp2	65,6 ± 13,8	25,2 ± 13,8	9,2 ± 6,0

4 Discussion

To the authors' knowledge, the flexible array of active concentric ring electrodes presented in this paper is the first one of these characteristics. Other authors have developed active concentric ring electrodes but on rigid substrates [3, 6–9]. This new sensor is more comfortable for the subject under study and provides a better contact since it adapts to the body surface curvature. Our group has recently developed other flexible concentric ring electrodes [19]. However such electrodes require the screen-printing of three layers, alternating conductor and dielectric pastes. In flexible substrates it is very complicated to use bias between layers, and the solution proposed in the present work favors an easier manufacturing. The comparison of the sensitivity of TCB opened-ring electrodes and closed-ring electrodes shown in this document reveals that signals can be picked up more attenuated with the opened-ring version, but with differences smaller than 3.8 % in the spatial distribution of the sensitivity. What is more, if a dielectric is used to prevent the contact between the skin and the conductive line that shortcuts the inner disc with the outer ring, these differences are smaller than 0.5 %. Regarding the model we used, it is more realistic than others [20] since it considers the abdominal layers with their different conductivities and thicknesses. It should also be pointed out that, in contrast to individual electrodes used in other studies [6–9, 19], the electrode array developed in this work is a more compact solution that reduces the signal preconditioning cost and space, and it is more suitable for bioelectrical mapping of the body surface. Furthermore, the modularity of the developed sensor permits to reuse the signal conditioning circuit while the sensing part can be disposed for hygienic reasons.

Signal recording experiences of this work show that active concentric electrodes of the flexible array enhance the quality of non-invasive EEnG signals in terms of electrocardiographic and respiratory interferences, in comparison to bipolar recordings with conventional disc electrodes. This is in agreement with previous studies that used this kind of electrodes implemented on rigid substrates [9]. The presence of these interferences is very common in non-invasive recordings of bioelectric signals and limits the bandwidth of analysis of such signals [21] with the corresponding loss of information. In order to cancel these physiological interferences many different signal-processing techniques have been developed [17, 22–24]. In contrast to these techniques, the electrode presented in this work permits to reduce such interferences in

the raw signals, with no need of post-processing and no computational cost which makes it ideal for real time monitoring applications. In the specific case of EEnG, on one hand, the reduction of respiratory interference permits to identify more easily the activity of intestinal slow wave [15]. On the other hand, the reduction of ECG interference could help the identification of spike bursts activity [17]. This could provide more robust systems to non-invasively monitor intestinal myoelectrical activity which could bring close the clinical application of this technique. Nevertheless, this should be confirmed in future studies.

Moreover, although it has not been tested in this work, according to other authors [25, 26], the Laplacian potential mapping can enhance spatial sensibility for surface bioelectrical activity. This can be of great importance for the studies of propagation maps of cardiac [27], electroencephalographic [28], intestinal [29] or uterine [30] activity which can provide electrophysiological information of clinical relevance. The developed flexible array of active concentric ring electrodes, with different electrode sizes, would be very suitable for these applications.

5 Conclusions

The flexible array of active concentric ring electrodes developed in this paper joins the benefits of Laplacian techniques in terms of enhancing spatial resolution, with the comfort and adaptation to body surface curvature of conventional disposable electrodes.

The non-invasive recordings of intestinal myolectrical signals with this new kind of electrodes provide enhanced bioelectric signals in terms of robustness to physiological interferences such as ECG and respiration, and permit to identify more easily the intestinal slow wave activity.

Acknowledgements. Research supported in part by the Ministerio de Ciencia y Tecnología de España (TEC 2010-16945) and by and by the Universidad Politècnica de València (SP20120469).

References

1. Bradshaw, L.A., Richards, W.O., Wikswo Jr., J.P.: Volume conductor effects on the spatial resolution of magnetic fields and electric potentials from gastrointestinal electrical activity. Med. Biol. Eng. Comput. **39**, 35–43 (2001)
2. Wu, D., Tsai, H.C., He, B.: On the estimation of the Laplacian electrocardiogram during ventricular activation. Ann. Biomed. Eng. **27**, 731–745 (1999)
3. Besio, W.G., Aakula, R., Koka, K., Dai, W.: Development of a tri-polar concentric ring electrode for acquiring accurate Laplacian body surface potentials. Ann. Biomed. Eng. **34**, 426–435 (2006)
4. Hjorth, B.: An on-line transformation of EEG scalp potentials into orthogonal source derivations. Electroencephalogr. Clin. Neurophysiol. **39**, 526–530 (1975)
5. Perrin, F., Pernier, J., Bertrand, O., Giard, M.H., Echallier, J.F.: Mapping of scalp potentials by surface spline interpolation. Electroencephalogr. Clin. Neurophysiol. **66**, 75–81 (1987)

6. Lu, C.C., Tarjan, P.P.: An ultra-high common-mode rejection ratio (CMRR) AC instrumentation amplifier for laplacian electrocardiographic measurement. Biomed. Instrum. Technol. **33**, 76–83 (1999)
7. Koka, K., Besio, W.G.: Improvement of spatial selectivity and decrease of mutual information of tri-polar concentric ring electrodes. J. Neurosci. Methods **165**, 216–222 (2007)
8. Li, G., Wang, Y., Jiang, W., Wang, L.L., Lu, C.-Y.S., Besio, W.G.: Active laplacian electrode for the data-acquisition system of EHG. J. Phys: Conf. Ser. **13**, 330–335 (2005)
9. Prats-Boluda, G., Garcia-Casado, J., Martinez-de-Juan, J.L., Ye-Lin, Y.: Active concentric ring electrode for non-invasive detection of intestinal myoelectric signals. Med. Eng. Phys. **33**, 446–455 (2011)
10. Quigley, E.M.: Gastric and small intestinal motility in health and disease. Gastroenterol. Clin. North Am. **25**, 113–145 (1996)
11. Weisbrodt, N.W.: Motility of the Small Intestine, 2nd edn, pp. 631–663. J. LR, New York (1987)
12. Fleckenstein, P., Oigaard, A.: Electrical spike activity in the human small intestine. A multiple electrode study of fasting diurnal variations. Am. J. Dig. Dis. **23**, 776–780 (1978)
13. Chen, J.D., Schirmer, B.D., McCallum, R.W.: Measurement of electrical activity of the human small intestine using surface electrodes. IEEE Trans. Biomed. Eng. **40**, 598–602 (1993)
14. Chang, F.Y., Lu, C.L., Chen, C.Y., Luo, J.C., Lee, S.D., Wu, H.C., Chen, J.Z.: Fasting and postprandial small intestinal slow waves non-invasively measured in subjects with total gastrectomy. J. Gastroenterol. Hepatol. **22**, 247–252 (2007)
15. Prats-Boluda, G., Garcia-Casado, J., Martinez-de-Juan, J.L., Ponce, J.L.: Identification of the slow wave component of the electroenterogram from Laplacian abdominal surface recordings in humans. Physiol. Meas. **28**, 1115–1133 (2007)
16. García-Casado, J., Martínez-de-Juan, J.L., Ponce, J.: Effect of abdominal layers on surface electroenterogram spectrum. In: Proceedings of the 25th Annual International Conference of the IEEE, vol. 3, pp. 2543–2546 (2003)
17. Garcia-Casado, J., Martinez-de-Juan, J.L., Ponce, J.L.: Adaptive filtering of ECG interference on surface EEnGs based on signal averaging. Physiol. Meas. **27**, 509–527 (2006)
18. Rush, S., Driscoll, D.A.: EEG electrode sensitivity–an application of reciprocity. IEEE Trans. Biomed. Eng. **16**, 15–22 (1969)
19. Prats-Boluda, G., Ye-Lin, Y., Ibañez, J., García-Breijo, E., García-Casado, J.: Active flexible concentric ring electrode for non invasive surface bioelectrical recordings. Meas. Sci. Technol. **23**, 10 (2012)
20. Besio, W.G., Koka, K., Aakula, R., Dai, W.: Tri-polar concentric ring electrode development for Laplacian electroencephalography. IEEE Trans. Biomed. Eng. **53**, 926 (2006)
21. Rabotti, C., Mischi, M., van Laar, J.O., Oei, G.S., Bergmans, J.W.: Inter-electrode delay estimators for electrohysterographic propagation analysis. Physiol. Meas. **30**, 745–761 (2009)
22. Irimia, A., Bradshaw, L.A.: Artifact reduction in magnetogastrography using fast independent component analysis. Physiol. Meas. **26**, 1059–1073 (2005)
23. Hassan, M., Boudaoud, S., Terrien, J., Karlsson, B., Marque, C.: Combination of canonical correlation analysis and empirical mode decomposition applied to denoising the labor electrohysterogram. IEEE Trans. Biomed. Eng. **58**, 2441–2447 (2011)
24. Vullings, R., Peters, C.H., Sluijter, R.J., Mischi, M., Oei, S.G., Bergmans, J.W.: Dynamic segmentation and linear prediction for maternal ECG removal in antenatal abdominal recordings. Physiol. Meas. **30**, 291–307 (2009)

25. Besio, W., Chen, T.: Tripolar Laplacian electrocardiogram and moment of activation isochronal mapping. Physiol. Meas. **28**, 515 (2007)
26. Soundararajan, V., Besio, W.: Simulated comparison of disc and concentric electrode maps during atrial arrhythmias. Int. J. Bioelectromagn. **7**, 217–220 (2005)
27. Haissaguerre, M., Hocini, M., Shah, A.J., Derval, N., Sacher, F., Jais, P., Dubois, R.: Noninvasive panoramic mapping of human atrial fibrillation mechanisms: a feasibility report. J. Cardiovasc. Electrophysiol. **24**, 711–717 (2013)
28. Hangya, B., Tihanyi, B.T., Entz, L., Fabo, D., Eross, L., Wittner, L., Jakus, R., Varga, V., Freund, T.F., Ulbert, I.: Complex propagation patterns characterize human cortical activity during slow-wave sleep. J. Neurosci. **31**, 8770–8779 (2011)
29. Lammers, W.J., Al-Bloushi, H.M., Al-Eisaei, S.A., Al-Dhaheri, F.A., Stephen, B., John, R., Dhanasekaran, S., Karam, S.M.: Slow wave propagation and plasticity of interstitial cells of Cajal in the small intestine of diabetic rats. Exp. Physiol. **96**, 1039–1048 (2011)
30. Rabotti, C., Mischi, M., Oei, S.G., Bergmans, J.W.: Noninvasive estimation of the electrohysterographic action-potential conduction velocity. IEEE Trans. Biomed. Eng. **57**, 2178–2187 (2010)